

$Y_2O_3:Eu^{3+}$ concentration and particle size: their impacts on color rendering index and lumen of multi-chip white diodes

Phuc Dang Huu¹, Phan Xuan Le²

¹Faculty of Fundamental Science, Industrial University of Ho Chi Minh City, Ho Chi Minh City, Vietnam

²Faculty of Mechanical-Electrical and Computer Engineering, School of Engineering and Technology, Van Lang University, Ho Chi Minh City, Vietnam

Article Info

Article history:

Received Oct 29, 2021

Revised Jun 4, 2022

Accepted Jun 25, 2022

Keywords:

Color rendering property

Extinction coefficient

Lambert-Beer law

Mie-scattering theory

$Y_2O_3:Eu^{3+}$

ABSTRACT

Aiming at achieving higher colour standard for multi-chip white light-emitting diode (MCW-LEDs) through the enhancement of their color rendering index (CRI), this article worked on and proposed a novel MCW-LED package using a compound of red phosphor $Y_2O_3:Eu^{3+}$. The red phosphors were synthesized and applied to build both protective coating and in-cup phosphor configurations. The CRI of MCW-LED which has high correlated colour heat of 8,500 K was observed to be heightened to 86. Moreover, the scattering of the light when added the red phosphor $Y_2O_3:Eu^{3+}$ is demonstrated using Mie-scattering theory, while the influences of the red-light enhancement is analyzed using the law of Lambert-Beer.

This is an open access article under the [CC BY-SA](https://creativecommons.org/licenses/by-sa/4.0/) license.



Corresponding Author:

Phan Xuan Le

Faculty of Mechanical-Electrical and Computer Engineering, School of Engineering and Technology

Van Lang University

Ho Chi Minh City, Vietnam

Email: le.px@vlu.edu.vn

1. INTRODUCTION

Multi-chip white light-emitting diode (MCW-LEDs) have been favoured in illumination market nowadays as their performance is much better than the standard lights like incandescent as well as fluorescent light bulbs. MCW-LEDs own outstanding features that can be listed as compact size, high brightness, low energy consumption and high durability even for outdoor use which probably lower the maintenance cost [1]-[3]. Not to mention, MCW-LEDs are safe for human health and environments as they do not release high heat during their operation time and do not have mercury in their packages. As a result, LEDs have been seen as a promising replacement to traditional light bulbs in terms of energy-efficient lighting solutions, and they may be widely employed in numerous parts of people's daily life such as industrial and commercial illumination, household lighting, as well as street lighting. To evaluate the quality of a MCW-LED, lumen efficiency and color uniformity or correlated color temperature (CCT) homogeneity are the two important factors which have been excessively studied for improvements. By adding a proper amount of SiO_2 phosphor powder into the light-emitting diode (LED) phosphor compound, the CCT deviation of the W-LED were minimized effectively while maintaining its luminescence value [4]-[6]. Besides, in an attempt to enhance the lumen output of W-LED packages, $Ce_{0.67} Tb_{0.33} MgAl_{11} O_{19}:Ce,Tb$ phosphorus particles were applied and achieved expected results [7]. Additionally, various studies on the color rendering indicator (CRI), a parameter commonly used for chromaticity evaluation of W-LEDs, have been conducted to heighten its value over 90. In previous researches of CRI enhancement, mixing or doping red phosphor material to the original

phosphor composition of LED package to increase the red-light components in the generated light was one of the most common methods [8], [9]. In the study of Won's research team, LED packages performing high CRI values were achieved by combining LED chips with the green and red phosphors of $(\text{Ba,Sr})_2\text{SiO}_4:\text{Eu}^{2+}$ and $\text{CaAlSiN}_3:\text{Eu}^{2+}$, respectively [10]. The colloidal quantum dot (QD) is another material using for accomplishing high-CRI W-LEDs. Chen and his partners applied the QD/polymethylmethacrylate (PMMA) combination to their phosphor-converted LEDs and successfully increased the CRI greater than 90 [11]-[14]. Obviously, the similarity of these studies is that they all aimed at high CRI while neglecting the luminous performance. Moreover, the WLED configurations used for analysis were the ones with single LED chip having 2,500-7,500 K CCT. Thus, they are not practical when being applied to fabricate WLEDs with multiple chips and higher CCTs such as 8,500 K. Europium-doped yttrium oxide ($\text{Y}_2\text{O}_3:\text{Eu}^{3+}$) phosphor is a luminescent material that has been largely applied to enhance the red-light components in white light generation [15]. $\text{Y}_2\text{O}_3:\text{Eu}^{3+}$ red phosphor is considered as one of the best red oxide phosphors because of its high thermal conductivity, chemical stability and color purity, as well as good corrosion resistance [16]-[18]. Yet, as far as we known, the effects of $\text{Y}_2\text{O}_3:\text{Eu}^{3+}$ on the CRI and illuminating beam of the MCW-LED have not been studied in depth. Therefore, the goal of our research is to analyze how $\text{Y}_2\text{O}_3:\text{Eu}^{3+}$ influences these two lighting properties of the MCW-LED using nine LED chips. The experiments are conducted on the two different WLED configurations, the protective coating phosphor and in-cup phosphor configurations. The research process in this article includes three stages, starting from developing the MCW-LED physical model having 8500 K CCT with LightTools 8.1.0 program, continuing with adding the $\text{Y}_2\text{O}_3:\text{Eu}^{3+}$ phosphors, and finishing with analysis and discussion of $\text{Y}_2\text{O}_3:\text{Eu}^{3+}$ effects on the CRI and luminescence properties of multi-chip LEDs emit white light. It is noted that the experiments were carried out with different concentrations and particle sizes of $\text{Y}_2\text{O}_3:\text{Eu}^{3+}$. The results demonstrated that $\text{Y}_2\text{O}_3:\text{Eu}^{3+}$ can help WLED get higher CRI and lumen output, depending on its applied concentration and particle sizes.

Our paper will contain four parts. Section 1 will explain why we choose the $\text{Y}_2\text{O}_3:\text{Eu}^{3+}$ phosphor to study. In section 2, the simulation of two MCW-LED models via LightTools program was presented. Subsequently, CRI and luminous efficiency of MCW-LED using $\text{Y}_2\text{O}_3:\text{Eu}^{3+}$ were analyzed and discussed in section 3. Finally, all the noticeable points of the research were summed up and showed in section 4.

2. RESEARCH METHOD

The simulation of the WLED package used for the investigation on the effects of red phosphor $\text{Y}_2\text{O}_3:\text{Eu}^{3+}$ was carried out based on the LightTools program, from which the simulated model is similar to the actual WLED package. The employed MCW-LED model is covered by flat silicone, as described in Figure 1. Besides, Figure 1 presented the information for an MCW-LED model got from Siliconware Precision Industries Co., Ltd., Taiwan [19], [20]. The experiments will be carried out on two different structures of LED packages and with various $\text{Y}_2\text{O}_3:\text{Eu}^{3+}$ concentrations and particle sizes. The conformal phosphor layout (CPP) as well as the in-cup phosphor layout (IPP) were simulated and demonstrated in Figure 2. The introduced CCT for these two packages is 8500 K. To meet the package's specifications, the CCT must be maintained at a stable level. This means that the concentration of $\text{YAG}:\text{Ce}^{3+}$ yellow phosphors should be reduced when $\text{Y}_2\text{O}_3:\text{Eu}^{3+}$ concentration increases.

CPP and IPP use the same reflectors, silicone lens and nine blue chips. The parameter of the reflector would be $2.07 \times 8 \times 9.85$ mm (depth x inner radius x outer radius). Every blue-color chip is 1.14×0.15 mm, emits 1.16 W radiant flux, and has the wavelength that peaks at 453 nm. Figure 2(a) presents the CPP with a 0.08-mm phosphor film coated conformally on the chips. Meanwhile, Figure 2(b) shows the IPP with the phosphor layer dispersed in the silicone lens and covering the LED chips. The phosphor layer in IPP is 2.07 mm thick and comprised of yellow $\text{YAG}:\text{Ce}$ phosphors, red $\text{Y}_2\text{O}_3:\text{Eu}^{3+}$ powders and the silicone matrix. The indicators of refraction of the silicone gel, $\text{YAG}:\text{Ce}$ and $\text{Y}_2\text{O}_3:\text{Eu}^{3+}$ phosphors are 1.50, 1.83 and 1.93, respectively. Besides, the phosphor particle size is $7.25 \mu\text{m}$, which is identical to the real size of a phosphor particle.



Lead frame: 4.7mm Jentech Size-S

LED chip: V45H

Die attach: Sumitomo 1295SA

Gold Wire: 1.0 mil

Phosphor: ITC NYAG4_EL

Figure 1. The 8,500 K MCW-LED and its specifications provided by the Siliconware Precision Industries Co., Ltd., Taiwan

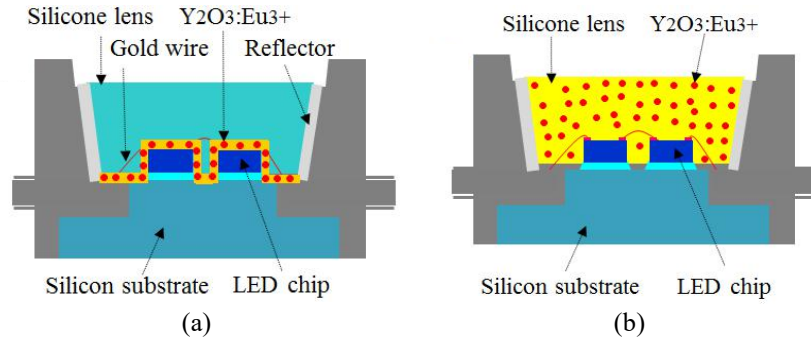


Figure 2. The two phosphor layouts in the MCW-LED device, (a) conformal phosphor layout (CPP) and (b) in-cup phosphor layout (IPP)

3. RESULTS AND ANALYSIS

The CRI and luminescence performances of MCW-LEDs with $Y_2O_3:Eu^{3+}$ based on the results of WLED simulation were examined and presented in this section. To examine the improvement of CRI, it is essential to keep average CCT of both CPP and IPP at 8,500 K while changing the concentration and particle sizes of $Y_2O_3:Eu^{3+}$ red phosphor. In both packages, the particle size of red phosphor ranges from 1 μm to 8 μm . Figure 3 presented the calculated CRI values of both CPP and IPP. Figure 3(a) showed that in the case of CPP configurations, the CRI went up continuously when the concentration of $Y_2O_3:Eu^{3+}$ increased from 0% to approximate 10% wt., regardless of the phosphor particle size. Besides, at $Y_2O_3:Eu^{3+}$ concentration varied from 8% to 16 % wt., the highest value of CRI which is over 86 can be observed at the particle size of 1 μm . The CRI of IPP displayed the same movement (Figure 3(b)). Particularly, with the concentration range of 0%-0.24%, the CRI showed a continuous growth at any phosphor diameter. As the concentration of the phosphor emits red light constantly increases 2.4%-0.32%, the CRI of IPP can reach its peak of 84 when 1 μm particle size is chosen. However, the decrease in CRI can be observed in either CPP or IPP cases, when $Y_2O_3:Eu^{3+}$ concentration and particle size exceeded a certain level, which is also demonstrated in Figure 3. The excessive red phosphor content means the red color is over-dominant and causes the degradation of CRI in both structures.

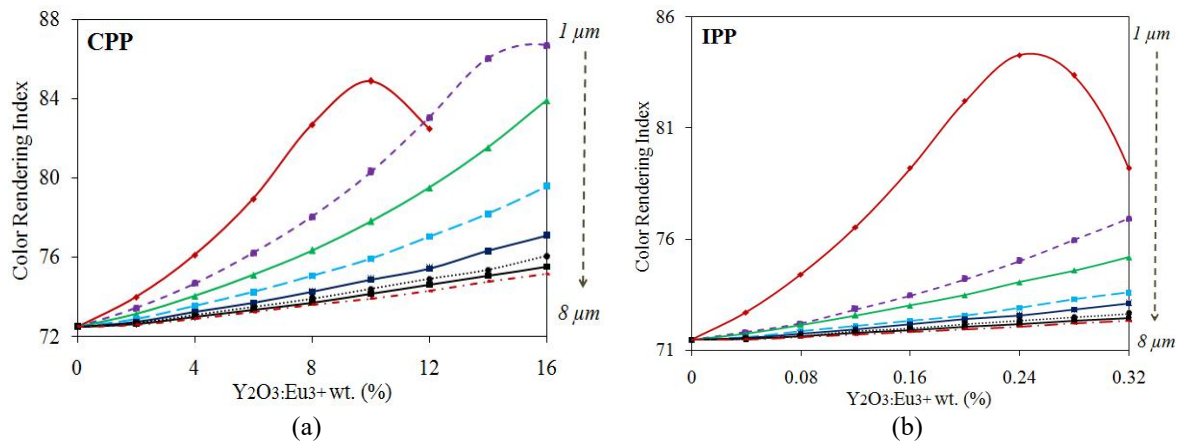


Figure 3. CRI under the median 8,500-K CCT as a function of $Y_2O_3:Eu^{3+}$ parameters in (a) CPP and (b) IPP

The emission spectra observed with different particle sizes (from 1 μm to 8 μm) and concentrations of $Y_2O_3:Eu^{3+}$ were demonstrated in Figure 4. Particularly, that of the CPP with 8% and 12% wt. $Y_2O_3:Eu^{3+}$ were displayed in turn in Figure 4(a) as well as (b). Meanwhile, Figures 4 (c) and (d) illustrated the results from the IPP using 0.16% and 0.24% wt. $Y_2O_3:Eu^{3+}$, respectively. Obviously, after the red phosphor $Y_2O_3:Eu^{3+}$ was added to the phosphor packages, the red-light spectral region in both conformal and in-cup structures increased, which is probably attributed to the enhancement of CRI.

Besides the CRI, the lighting yield of the protective coating and in-cup phosphor structures when using red phosphor $Y_2O_3:Eu^{3+}$ with different concentrations and diameters was examined and shown in

Figure 5. Figures 5(a) and (b) are the attained figures for conformal structure while that of the in-cup package can be observed in Figures 5(c) and (d). Figures 5(a)-(d) all declared that as the lower concentration of $Y_2O_3:Eu^{3+}$ was applied, the extinction coefficient decreased, leading to a higher luminous output. It can be also said that the luminous efficacy rises with the increase of $Y_2O_3:Eu^{3+}$ size owing to the extinction-coefficient reduction.

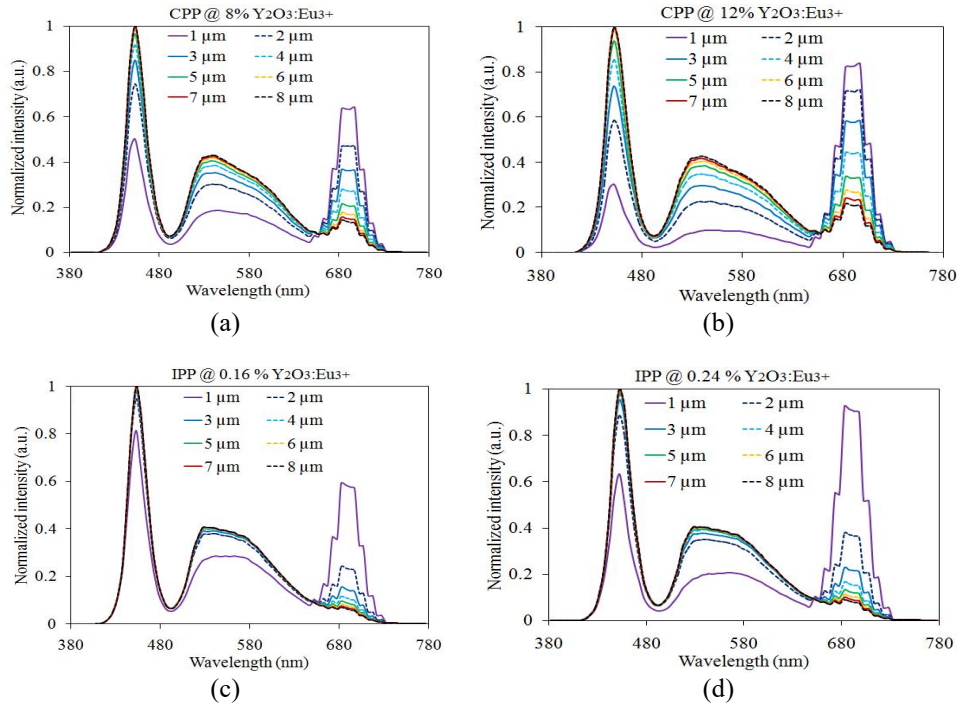


Figure 4. Emission spectra in several phosphors under different $Y_2O_3:Eu^{3+}$ contents (a) 8%, (b) 12% (for CPP layout), (c) 0.16%, and (d) 0.24% (for IPP layout)

Mie-scattering theory was utilized to investigate the connection between the $Y_2O_3:Eu^{3+}$ particle size and the lighting productivity of MCW-LEDs, by which the attained results can be verified [21], [22]. The Lambert-Beer law was also utilized to calculate lighting attenuation:

$$I = I_0 \exp(-\mu_{ext}L) \tag{1}$$

where I and I_0 are the transmitted and incident light power, respectively. μ_{ext} shows the extinction factor, and L presents the path lengthiness. Besides, the extinction coefficient μ_{ext} could be calculated by $\mu_{ext} = N \cdot C_{ext}$ with N being the amount of granules for each cubic millimeter, and C_{ext} being the extinction cross section for granules of phosphor. By using Mie theory [23]-[25], C_{ext} can be expressed as:

$$C_{ext} = \frac{2\pi a^2}{x^2} \sum_{n=1}^{\infty} (2n + 1) \text{Re}(a_n + b_n) \tag{2}$$

$x = 2\pi a / \lambda$ will be the size of the phosphor sphere; a_n and b_n will be the development factors having even and odd symmetries, respectively, and are demonstrated as:

$$a_n(x, m) = \frac{\psi'_n(mx)\psi_n(x) - m\psi_n(mx)\psi'_n(x)}{\psi_n(mx)\xi_n(x) - m\psi_n(mx)\xi'_n(x)} \tag{3}$$

$$b_n(x, m) = \frac{m\psi'_n(mx)\psi_n(x) - \psi_n(mx)\psi'_n(x)}{m\psi_n(mx)\xi_n(x) - \psi_n(mx)\xi'_n(x)} \tag{4}$$

here, a shows the particle radius, λ indicates the comparative diffusing wavelength, m presents the indicator of refraction of diffusing granules. $\Psi_n(x)$ and $\xi_n(x)$ are the functions of Riccati-Bessel.

The analysis of extinction coefficient in CPP and IPP are carried out at the emission peak wavelength of YAG:Ce yellow phosphor (555 nm) and the blue LED chip (453 nm). The luminescence results of CPP in Figures 5(a) and (b) were compared with the ones of IPP in Figures 5(c) and (d). From the

comparison, it can be concluded that high luminous efficiency can be obtained at lower concentration and with larger particle size of $Y_2O_3:Eu^{3+}$ because in these cases, the extinction coefficient values were reduced. These results are the valuable information that can be useful in investigating the influences of $Y_2O_3:Eu^{3+}$ diameters and concentrations on the MCW-LEDs luminous performance.

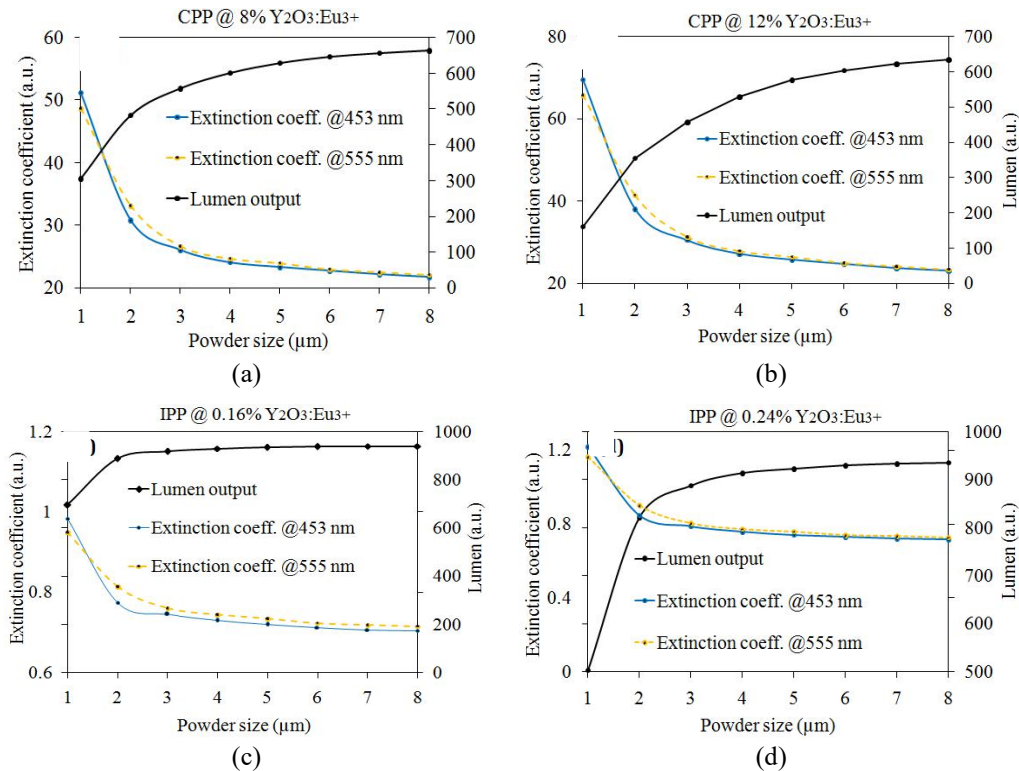


Figure 5. The lumen output along with the calculated extinction coefficient under different $Y_2O_3:Eu^{3+}$ contents (a) 8%, (b) 12% (for CPP layout), (c) 0.16%, and (d) 0.24% (for IPP layout)

4. CONCLUSION

The article presented the impacts of the particles of phosphor $Y_2O_3:Eu^{3+}$ emits red light upon the CRI and the luminescent properties of both conformal and in-cup phosphor MCW-LEDs as a function of $Y_2O_3:Eu^{3+}$ concentrations and particle sizes. The improvement of CRI was observed in two phosphor structures when the red $Y_2O_3:Eu^{3+}$ phosphor in the packages; specifically, the highest CRI of the conformal structure is 86 when using approximate 10% $Y_2O_3:Eu^{3+}$ with the particle size of 1 μm , while the in-cup structure can yield the best CRI of 84 at 0.24 % concentration and 1 μm particle size of $Y_2O_3:Eu^{3+}$. On the other hand, CRI decreases when the particle magnitude of $Y_2O_3:Eu^{3+}$ increases. Regarding the lumen efficiency, the results indicated that it can be enhanced by using $Y_2O_3:Eu^{3+}$ with a lower concentration and a larger particle size because in both cases the extinction coefficient was reduced significantly. These results can prove that $Y_2O_3:Eu^{3+}$ red phosphor is an appropriate phosphor material for fabricating MCW-LEDs with high CRI and luminous performance, which greatly supports the further development of MCW-LEDs manufacturing.

ACKNOWLEDGEMENTS

This study was financially supported by Van Lang University, Vietnam.




REFERENCES

- [1] N. Bamiedakis *et al.*, "Ultra-low cost high-density two-dimensional visible-light optical interconnects," *Journal of Lightwave Technology*, vol. 37, no. 13, pp. 3305–3314, Jul. 2019, doi: 10.1109/JLT.2019.2914310.
- [2] A. Ahmad, A. Kumar, V. Dubey, A. Butola, B. S. Ahluwalia, and D. S. Mehta, "Characterization of color cross-talk of CCD detectors and its influence in multispectral quantitative phase imaging," *Optics Express*, vol. 27, 2019, doi: 10.1364/oe.27.004572.
- [3] T. Shao *et al.*, "Understanding the role of fluorine-containing plasma on optical properties of fused silica optics during the combined process of RIE and DCE," *Optics Express*, vol. 27, no. 16, p. 23307, Aug. 2019, doi: 10.1364/oe.27.023307.




- [4] T. P. White, E. Deleporte, and T.-C. Sum, "Feature issue introduction: halide perovskites for optoelectronics," *Optics Express*, vol. 26, no. 2, p. A153, Jan. 2018, doi: 10.1364/oe.26.00a153.
- [5] H. Kim, Y.-J. Seo, and Y. Kwak, "Transparent effect on the gray scale perception of a transparent OLED display," *Optics Express*, vol. 26, no. 4, p. 4075, Feb. 2018, doi: 10.1364/oe.26.004075.
- [6] D. Durmus and W. Davis, "Blur perception and visual clarity in light projection systems," *Optics Express*, vol. 27, no. 4, p. A216, Feb. 2019, doi: 10.1364/oe.27.00a216.
- [7] C. Tian *et al.*, "Mn⁴⁺ activated Al₂O₃ red-emitting ceramic phosphor with excellent thermal conductivity," *Optics Express*, vol. 27, no. 22, p. 32666, Oct. 2019, doi: 10.1364/oe.27.032666.
- [8] Y. Shi, S. Ye, J. Yu, H. Liao, J. Liu, and D. Wang, "Simultaneous energy transfer from molecular-like silver nanoclusters to Sm³⁺/Ln³⁺ (Ln = Eu or Tb) in glass under UV excitation," *Optics Express*, vol. 27, no. 26, Dec. 2019, doi: 10.1364/oe.380860.
- [9] J. Li, Y. Tang, Z. Li, X. Ding, L. Rao, and B. Yu, "Investigation of stability and optical performance of quantum-dot-based LEDs with methyl-terminated-PDMS-based liquid-type packaging structure," *Optics Letters*, vol. 44, no. 1, 2019, doi: 10.1364/ol.44.000090.
- [10] S. An, J. Zhang, and L. Zhao, "Optical thermometry based on upconversion luminescence of Yb³⁺-Er³⁺ and Yb³⁺-Ho³⁺ doped Y₆WO₁₂ phosphors," *Applied Optics*, vol. 58, no. 27, p. 7451, Sep. 2019, doi: 10.1364/ao.58.007451.
- [11] J.-S. Li, Y. Tang, Z.-T. Li, L.-S. Rao, X.-R. Ding, and B.-H. Yu, "High efficiency solid-liquid hybrid-state quantum dot light-emitting diodes," *Photonics Research*, vol. 6, no. 12, p. 1107, Dec. 2018, doi: 10.1364/prj.6.001107.
- [12] S. Jost, C. Cauwerts, and P. Avouac, "CIE 2017 color fidelity index Rf: a better index to predict perceived color difference?," *Journal of the Optical Society of America A*, vol. 35, no. 4, p. B202, Apr. 2018, doi: 10.1364/josaa.35.00b202.
- [13] K. Chung, J. Sui, T. Sarwar, and P.-C. Ku, "Feasibility study of nanopillar LED array for color-tunable lighting and beyond," *Optics Express*, vol. 27, no. 26, p. 38229, Dec. 2019, doi: 10.1364/oe.382287.
- [14] S. Pan, B. Yang, X. Xie, and Z. Yun, "Image restoration and color fusion of digital microscopes," *Applied Optics*, vol. 58, no. 9, p. 2183, Mar. 2019, doi: 10.1364/ao.58.002183.
- [15] Z. Li, J. Zheng, J. Li, W. Zhan, and Y. Tang, "Efficiency enhancement of quantum dot-phosphor hybrid white-light-emitting diodes using a centrifugation-based quasi-horizontal separation structure," *Optics Express*, vol. 28, 2020, doi: 10.1364/oe.392900.
- [16] V. Bahrami-Yekta and T. Tiedje, "Limiting efficiency of indoor silicon photovoltaic devices," *Optics Express*, vol. 26, no. 22, p. 28238, Oct. 2018, doi: 10.1364/oe.26.028238.
- [17] S. Lee *et al.*, "Printed cylindrical lens pair for application to the seam concealment in tiled displays," *Optics Express*, vol. 26, no. 2, p. 824, Jan. 2018, doi: 10.1364/oe.26.000824.
- [18] R. Deeb, J. Van de Weijer, D. Muselet, M. Hebert, and A. Tremeau, "Deep spectral reflectance and illuminant estimation from self-interreflections," *Journal of the Optical Society of America A*, vol. 36, no. 1, p. 105, Jan. 2019, doi: 10.1364/josaa.36.000105.
- [19] C.-H. Lin *et al.*, "Hybrid-type white LEDs based on inorganic halide perovskite QDs: candidates for wide color gamut display backlights," *Photonics Research*, vol. 7, no. 5, p. 579, May 2019, doi: 10.1364/prj.7.000579.
- [20] K. Werfli *et al.*, "Experimental demonstration of high-speed 4 × 4 imaging multi-CAP MIMO visible light communications," *Journal of Lightwave Technology*, vol. 36, no. 10, pp. 1944–1951, May 2018, doi: 10.1109/JLT.2018.2796503.
- [21] Y. Zhang, J. Wang, W. Zhang, S. Chen, and L. Chen, "LED-based visible light communication for color image and audio transmission utilizing orbital angular momentum superposition modes," *Optics Express*, vol. 26, no. 13, 2018, doi: 10.1364/oe.26.017300.
- [22] X. Ding *et al.*, "Improving the optical performance of multi-chip LEDs by using patterned phosphor configurations," *Optics Express*, vol. 26, no. 6, p. A283, Mar. 2018, doi: 10.1364/oe.26.00a283.
- [23] H. Liu, Y. Shi, and T. Wang, "Design of a six-gas NDIR gas sensor using an integrated optical gas chamber," *Optics Express*, vol. 28, no. 8, p. 11451, Apr. 2020, doi: 10.1364/oe.388713.
- [24] C. Jaques, E. Pignat, S. Calinon, and M. Liebling, "Temporal super-resolution microscopy using a hue-encoded shutter," *Biomedical Optics Express*, vol. 10, no. 9, p. 4727, Sep. 2019, doi: 10.1364/boe.10.004727.
- [25] M. Royer, "Evaluating tradeoffs between energy efficiency and color rendition," *OSA Continuum*, vol. 2, no. 8, p. 2308, Aug. 2019, doi: 10.1364/osac.2.002308.

BIOGRAPHIES OF AUTHORS



Phuc Dang Huu    received a Physics Ph.D degree from the University of Science, Ho Chi Minh City, in 2018. Currently, he is a lecturer at the Faculty of Fundamental Science, Industrial University of Ho Chi Minh City, Ho Chi Minh City, Vietnam. His research interests include simulation LEDs material, renewable energy. He can be contacted at email: danghuuphuc@iuh.edu.vn.



Phan Xuan Le    received a Ph.D. in Mechanical and Electrical Engineering from Kunming University of Science and Technology, Kunming City, Yunnan Province, China. Currently, he is a lecturer at the Faculty of Engineering, Van Lang University, Ho Chi Minh City, Viet Nam. His research interests are optoelectronics (LED), power transmission and automation equipment. He can be contacted at email: le.px@vlu.edu.vn.